Exploring water-soluble organic aerosols structures in urban atmosphere using

advanced solid-state ¹³C NMR spectroscopy

3

1

2

- 4 Regina M. B. O. Duarte ^a *, Pu Duan ^b, Jingdong Mao ^c, Wenying Chu ^c, Armando C. Duarte ^a, Klaus
- 5 Schmidt-Rohr b

6

- 7 a Department of Chemistry & CESAM, University of Aveiro, 3810-193, Aveiro, Portugal
- 8 b Department of Chemistry, Brandeis University, 415 South Street, Waltham, MA 02453, USA
- 9 ° Department of Chemistry and Biochemistry, Old Dominion University, 4541 Hampton Blvd, Norfolk, VA
- 10 23529, USA

11

12

* Corresponding author: E-mail: regina.duarte@ua.pt; Phone: +351 234 370 200.

13 14

15

16

17

18

19

20

21

22

23

24

25

26

27

28

29

30

Abstract: Water-soluble organic matter (WSOM) in air particles has profound effects on climate and human health. At the heart of this environmental significance of WSOM lies a complex set of compounds, of which a major fraction still often remains undeciphered. Yet, not all environmental problems require delving into the molecular-level identification of WSOM constituents. Understanding the contribution of different functional groups to whole aerosol WSOM composition offers a highly important structural dataset that enables a better representation of WSOM in climate studies. For the first time, advanced solid-state ¹³C nuclear magnetic resonance (NMR) techniques, including nearly quantitative ¹³C multiple cross polarization/magic angle spinning (multiCP/MAS), multiCP/MAS with dipolar dephasing, multiCP/MAS with ¹³C chemical shift anisotropy filter, and two-dimensional ¹H-¹³C heteronuclear correlation (2D HETCOR), are applied to acquire an accurate quantitative structural description of whole aerosol WSOM collected in an urban atmosphere. Two urban aerosol WSOM samples collected in two short periods of time, under different wintry weather conditions, were investigated. NMR data successfully pinpointed the variability of whole aerosol WSOM composition, allowing to suggest source-specific structural characteristics for each sample in two short periods of time. A new structural model of urban aerosol WSOM was build based on this compositional data, showing the presence of three independent classes of compounds that vary both in content and

molecular diversity within short periods of time: heteroatom-rich aliphatic (either chain or branched), carbohydrate-like moieties, and highly substituted aromatic units. These findings establish advanced solid-state NMR as a promising tool for probing the chemical structures of inhomogeneous aerosol WSOM in rapidly changing atmospheric conditions, allowing to resolve discrepancies between modeled and measured aerosol WSOM.

36

37

38

31

32

33

34

35

Keywords: Water-soluble organic aerosols; Quantitative structural diversity; Structural model; Source assignment; Advanced solid-state ¹³C NMR spectroscopy

39

40

41

42

43

44

45

46

47

48

49

50

51

52

53

54

55

56

57

58

59

60

1. Introduction

Water-soluble organic matter (WSOM) from fine particulate matter (PM_{2.5}, aerodynamic diameter less than 2.5 µm) plays a key role on climate, through its impact on cloud formation and properties (Müller et al., 2017; Padró et al., 2010), Earth's radiative balance (Laskin et al., 2015; Moise et al., 2015), and atmospheric chemistry (George et al., 2015; Laskin et al., 2015). Atmospheric deposition of aerosol WSOM can also affect carbon and nitrogen biogeochemical cycles in aquatic ecosystems (lavorivska et al., 2016; Witkowska et al., 2016). Fine aerosol WSOM may also exert adverse health effects by generating reactive oxygen and nitrogen species (Tuet et al., 2016; Verma et al., 2014). Understanding these dynamic processes involving aerosol WSOM depends on how well one can identify its organic constituents. Yet, the ability to address such organic matrix is rather challenging, including PM_{2.5} collection in amounts suitable for chemical analysis, WSOM extraction/processing ensuring representativeness of the extracted organic materials, complexity of WSOM composition, and limitations of some instrumental techniques to deal with such complexity (Duarte and Duarte, 2011). Keeping these challenges in mind, one must decide the level of structural and/or molecular knowledge required to answer a specific problem. In fact, most of the research on aerosol WSOM (e.g., optical properties, secondary formation, atmospheric variability, and source apportionment) only require intermediate levels of structural analysis, such as the identification of specific classes of compounds or functional groups (Nozière et al., 2015). Still, attaining this level of structural identification necessitates an understanding of the inherent complexity of WSOM composition, as well as its atmospheric fate and reactivity (Duarte and Duarte, 2015; Nozière et al., 2015).

Recent reviews have settled the debate regarding the use of different sophisticated analytical techniques to unravel the complex chemical composition of aerosol WSOM (Duarte and Duarte, 2017; Nozière et al., 2015). The remarkable advance of high-resolution analytical techniques, namely ultrahigh resolution mass spectrometry and solution-state multidimensional nuclear magnetic resonance (NMR) spectroscopy, has provided fundamentally novel insights into the structural composition of aerosol WSOM (Chalbot et al., 2013, 2016; Duarte et al., 2019, 2017a; Duarte and Duarte, 2017, 2011; Matos et al., 2017; Schmitt-Kopplin et al., 2010; Willoughby et al., 2016). Solution-state NMR methods have been particularly essential in clarifying some intricacies of the structure-origin relationships of different aerosol WSOM samples. However, these methods still have several shortcomings when dealing with complex organic mixtures (e.g., low sample solubility, non-detection of non-protonated carbons). A more comprehensive overview on these limitations is found in Simpson et al., (Simpson et al., 2011) and Mao et al. (Mao et al., 2017). Solid-state ¹³C NMR, on the other hand, is an essential tool in overcoming some of those limitations in the untargeted structural analysis of complex mixtures (Mao et al., 2017). As described by Mao and co-workers (2017), when compared with solution-state NMR, solid-state NMR has the following advantages: (1) it overcomes sample solubility problems; (2) it requires less sample handling and is free of solvent effects; (3) it does not consume sample, thus allowing for its recovery for subsequent structural analysis; (4) it facilitates a much higher sample concentration than solution NMR, thus enhancing signals intensity; (5) it allows the straightforward detection of non-protonated carbons, allowing for the quantitative characterization of complex organic matrices; (6) the fast tumbling of molecules averages anisotropic interactions in solution NMR, while in solid-state NMR these anisotropic interactions can be manipulated with specially developed pulse sequences to extract structural information not available from solution NMR; (7) it can identify domains and heterogeneities within complex organic structures, which cannot be easily discerned by solution NMR; and (8) the macromolecular structures, aggregates, and colloids present in complex organic mixtures slow the tumbling of these molecules, leading to T_2 relaxation times that are too short to allow many of the pulse sequences of solution NMR to be successfully used (Mao et al., 2017). Yet, the application of solid-state ¹³C NMR to aerosol WSOM analysis has been rather limited (Duarte et al., 2015, 2007; Sannigrahi et al., 2006), mostly due to the low atmospheric concentrations of aerosol WSOM, rendering the routine application of these methods difficult. When solid-state ¹³C NMR is used for aerosol WSOM characterization, the individual WSOM samples are usually pooled together

61

62

63

64

65

66

67

68

69

70

71

72

73

74

75

76

77

78

79

80

81

82

83

84

85

86

87

88

89

according to different pollution or seasonal events, aiming at obtain enough amount of sample for NMR analysis (30-80 mg) (Duarte et al., 2015, 2007, 2005; Sannigrahi et al., 2006). These composite aerosol WSOM samples typically represent average ambient and/or meteorological conditions (e.g. seasons or biomass burning events), which however do not allow for capturing the individual WSOM compositional changes in short periods of time (i.e., up to a week (Duarte and Duarte, 2017)), thus hindering the investigation of chemical processes or aerosol sources in rapidly changing scenarios (e.g., different air masses or changes in atmospheric boundary-layer height). Furthermore, the most frequently used technique has been the standard cross-polarization magic-angle spinning (CP/MAS) 13C NMR experiment, which only provides a semi-quantitative assessment of the carbon functional group distributions within the studied samples. Advanced solid-state ¹³C NMR methods (e.g., ¹³C direct polarization/magic angle spinning (DP/MAS) and DP/MAS with recoupled dipolar dephasing, ¹³C multiple cross polarization/MAS (multiCP/MAS) and multiCP/MAS with dipolar dephasing, ¹³C chemical shift anisotropy (CSA) filter, and two-dimensional ¹H-¹³C heteronuclear correlation (2D HETCOR) NMR) can cope with this complexity by successfully providing accurate and detailed structural data on complex organic mixtures, such as those from aquatic and soil samples. In this regard, readers are encouraged to consult the works of Johnson and Schmidt-Rohr (2014) and Mao et al. (2017, 2012, 2011), and references therein to obtain a more complete understanding of the advantages of advanced solid-state ¹³C NMR methods over conventional CP/MAS ¹³C NMR for the analysis of such complex organic materials (Johnson and Schmidt-Rohr, 2014; Mao et al., 2017, 2012, 2011). These advanced solid-state NMR methods have never been applied to the structural analysis of aerosol WSOM. Furthermore, little is known about the structural features of the aerosol WSOM as a whole, as an important fraction of this organic component still eludes the current analytical window. This study took the challenge to explore the structural diversity of whole aerosol WSOM by applying for the first time advanced solid-state ¹³C NMR techniques. A standard reference sample of urban air particles (NIST SRM® 1648a) and urban PM_{2.5} WSOM samples collected under different weather conditions during two consecutive weeks in winter were selected for this study. The NIST SRM® 1648a material was used as a surrogate for urban PM_{2.5} samples to assess whether the whole atmospheric particulate matter was amenable to advanced solid-state ¹³C NMR analysis. The objectives were: (i) to assess the effectiveness of advanced solid-state ¹³C NMR for the analysis of organic aerosols, (ii) to acquire a comprehensive structural description of whole aerosol WSOM, (iii) to quantify and assess the

91

92

93

94

95

96

97

98

99

100

101

102

103

104

105

106

107

108

109

110

111

112

113

114

115

116

117

118

119

variability of the structural composition of whole aerosol WSOM in two short periods of time, (iv) to identify the potential sources of the major structural categories of aerosol WSOM, and (v) to build structural model representing the chemical diversity of urban aerosol WSOM. The level of structural details here attained breaks the solid-state NMR resolution barrier on the spectral identification of specific chemical classes in ambient organic aerosols, allowing the accurate assessment of the atmospheric concentrations of the major and specific functional groups of these highly complex atmospheric matrices on relatively short periods of time.

128

129

130

131

132

133

134

135

136

137

138

139

140

141

142

143

144

145

146

147

148

149

150

121

122

123

124

125

126

127

2. Materials and methods

2.1. Sampling and extraction of aerosol WSOM samples

The PM_{2.5} samples were collected on a rooftop (ca. 20 m above ground) at the campus of University of Aveiro (40°38'N, 8°39'W), which is located about 10 km from the Atlantic coast on the outskirts of the city of Aveiro. The sampling site is impacted by both marine air masses travelling from the Atlantic Ocean and anthropogenic emissions from vehicular transport, residential, and industrial sources (Duarte et al., 2019, 2017b; Matos et al., 2017). Episodes of increased PM_{2.5} and WSOM concentrations are common in this area during colder seasons and they can last several days (Duarte et al., 2019, 2017b, 2015), allowing the collection of enough amount of aerosol WSOM within relatively short periods of time for subsequent NMR studies. Each PM_{2.5} sample was collected on a weekly basis (i.e., 7 days in continuum) in the periods of 4-11 February 2015 (Sample S1, start/end time: 15:35) and 11-18 February 2015 (Sample S2, start/end time: 15:50), on pre-fired (at 500 °C) quartz-fiber filters (20.3×25.4 cm; Whatman QM-A, Maidstone, UK) with an airflow rate of 1.13 m³ min⁻¹. Additional details on aerosol sampling procedure are available in Section S1, in Supplementary Material (SM) data. After sampling, the filter samples were folded in two, wrapped in aluminum foil and immediately transported to the laboratory, where they were weighted and stored frozen until further analysis. The meteorological data recorded during the PM_{2.5} samples collection are available in Table S1, in SM. An area of 315 cm² of each collected filter was extracted with 150 mL of ultra-pure water, and the dissolved organic carbon (DOC) content of each aqueous extract was measured by means of a Shimadzu (Kyoto, Japan) TOC-5000A Analyzer. Additional details on water-soluble organic carbon (WSOC) extraction and DOC analysis can be found in Section S2, in the SM. The WSOC concentrations are expressed in µg C m⁻³ (additional details are available in Table S2, in SM). After the WSOC

extraction, each aqueous aerosol extract was freeze-dried, and the obtained solid residues (designated as "whole aerosol WSOM samples") were kept in a desiccator over silica gel until the solid-state NMR analysis.

154

155

156

157

158

159

160

161

162

163

164

165

166

167

168

169

170

171

172

173

174

175

176

177

178

179

180

151

152

153

2.2. Advanced solid-state ¹³C NMR spectroscopy

All the NMR experiments were performed at 100 MHz for ¹³C and 400 MHz for ¹H using a Bruker Avance 400 spectrometer. Solid NIST SRM® 1648a material and aerosol WSOM samples were packed in 4mm-diameter zirconia rotors with Kel-F caps, and experiments were run in a double-resonance probe head. The ¹³C chemical shifts were referenced externally to tetramethylsilane (TMS), with ¹³COO⁻ labeled glycine at 176.49 ppm as a secondary reference. Quantitative ¹³C NMR spectra were acquired using direct polarization (DP), 14 kHz magic-angle spinning (MAS), and a recycle delay of 20 s for NIST SRM® 1648a (approximately 90 mg), 1 s for aerosol WSOM sample S1 (approximately 32 mg), and 4 s for aerosol WSOM sample S2 (approximately 80 mg). The acquired ¹³C DP/MAS NMR spectra are shown in Section S3, Figure S1, in the SM. Urban aerosol WSOM samples S1 and S2 were further characterized using nearly quantitative multiple cross-polarization magic angle spinning (multiCP/MAS) ¹³C NMR, multiCP/MAS ¹³C NMR with dipolar dephasing, and multiCP/MAS with a ¹³C chemical shift anisotropy (CSA) filter. The nearly quantitative multiCP/MAS ¹³C spectra were collected at a spinning speed of 14 kHz, with very small (<3%) spinning sidebands that have minimal overlap with centerbands. The 90° ¹³C pulse length was 4.2 μs (Johnson and Schmidt-Rohr, 2014). The multiCP/MAS experiment combined with dipolar dephasing was applied to obtain quantitative structural information on nonprotonated carbons and mobile segments. Most of the experimental conditions were the same as for the multiCP/MAS method except that a recoupled dipolar dephasing time of 68 µs was applied (Mao and Schmidt-Rohr, 2004a). The ¹³C CSA filter was used to separate signals of sp³-hybridized carbons from those of sp2- and sp-hybridized carbons (i.e., to resolve the overlap between anomeric and aromatic carbon signals). This technique is based on the carbon bonding symmetry, which results in CSAs of sp³-hybridized carbons being much smaller than those of sp²- and sp-hybridized carbons, so their magnetization remains after a certain recoupling time (Mao and Schmidt-Rohr, 2004b). Sample S2 was further characterized by means of two-dimensional ¹H-¹³C heteronuclear correlation (2D HETCOR) NMR. In the 2D HETCOR spectrum, specific functional groups and their connectivities and proximity can be identified (Mao et al., 2001). 2D HETCOR experiments were performed at a spinning speed of 7.5 kHz. Standard Hartmann-Hahn CP (HH-CP) with 0.5 ms CP time was used, allowing for correlations between carbons and protons within ~0.5 nm radius. Sample S1 was not analyzed by means of 2D HETCOR due to its small mass amount (approximately 32 mg) and correspondingly low signal-to-noise ratio.

3. Results and discussion

3.1. Contribution of WSOM to PM_{2.5} mass

The ambient concentrations of PM_{2.5}, water-soluble organic carbon (WSOC), and total mass of WSOM follow the same weekly trend, with higher values during the first week (Table 1). During this period, the inflowing air masses mostly come from inland (Table S1, SM), containing presumably a higher content of particulate organics from both local and continental sources. These conditions contrast with the cleaner air masses originating from the ocean sector during the second week, which usually contain a lower amount of particulate organic matter. Overall, the WSOM accounts to 23.4-25.3% of the urban PM_{2.5} mass during the two sampling periods, being within the range of variation previously reported for this same location in winter (Duarte et al., 2017a).

Table 1. Ambient concentrations of PM_{2.5}, WSOC, total mass of particulate WSOM, and WSOM/PM_{2.5} mass ratio in each sampling period.

Parameter	Sample S1	Sample S2		
Total PM _{2.5} (μg m ⁻³)	22.7	16.9		
WSOC (μg C m ⁻³)	3.32 ± 0.08	2.67 ± 0.04		
WSOM ^(a) (μg m ⁻³)	5.31 ± 0.26	4.28 ± 0.10		
WSOM/PM _{2.5} (%)	23.4	25.3		

 $^{^{(}a)}$ [WSOM] = [WSOC] \times 1.6 (factor used to convert WSOC into WSOM derived from elemental analysis of WSOC aerosol samples collected during different seasons at Aveiro (Duarte et al., 2015)).

3.2. Qualitative and quantitative NMR analysis of aerosol WSOM

Figures 1(a) and 1(b) shows the nearly quantitative multiple cross-polarization magic angle spinning (multiCP/MAS) ¹³C NMR spectra of aerosol WSOM samples S1 and S2, respectively. The corresponding dipolar-dephased 68-μs ¹³C multiCP/MAS NMR spectra are shown in Figures 1(c) and 1(d), whereas the ¹³C multiCP/MAS spectra after a 13C chemical shift anisotropy (CSA) filter are displayed in Figures 1(e) and 1(f). The quantitative direct polarization magic angle spinning (DP/MAS)

¹³C NMR spectra of the aerosol WSOM samples and NIST SRM® 1648a material are shown in Figure S1 (SM). The higher noise level in the DP spectra, particularly of sample S1, hinders the detection of smaller peaks, which are more clearly observed in the corresponding multiCP spectra due to their better signal-to-noise ratio. The presence of large spinning sidebands in the DP spectrum of NIST SRM® 1648a, which are also seen in the corresponding ¹H NMR spectrum (Figure S2, SM), are likely due to dipolar fields of paramagnetic species in this sample; this is supported by the presence of iron in the sample (3.92 ± 0.21%, certified mass fraction). This feature indicates the need to minimize the amount of paramagnetic species in the sample, which is the case for WSOM samples S1 and S2.

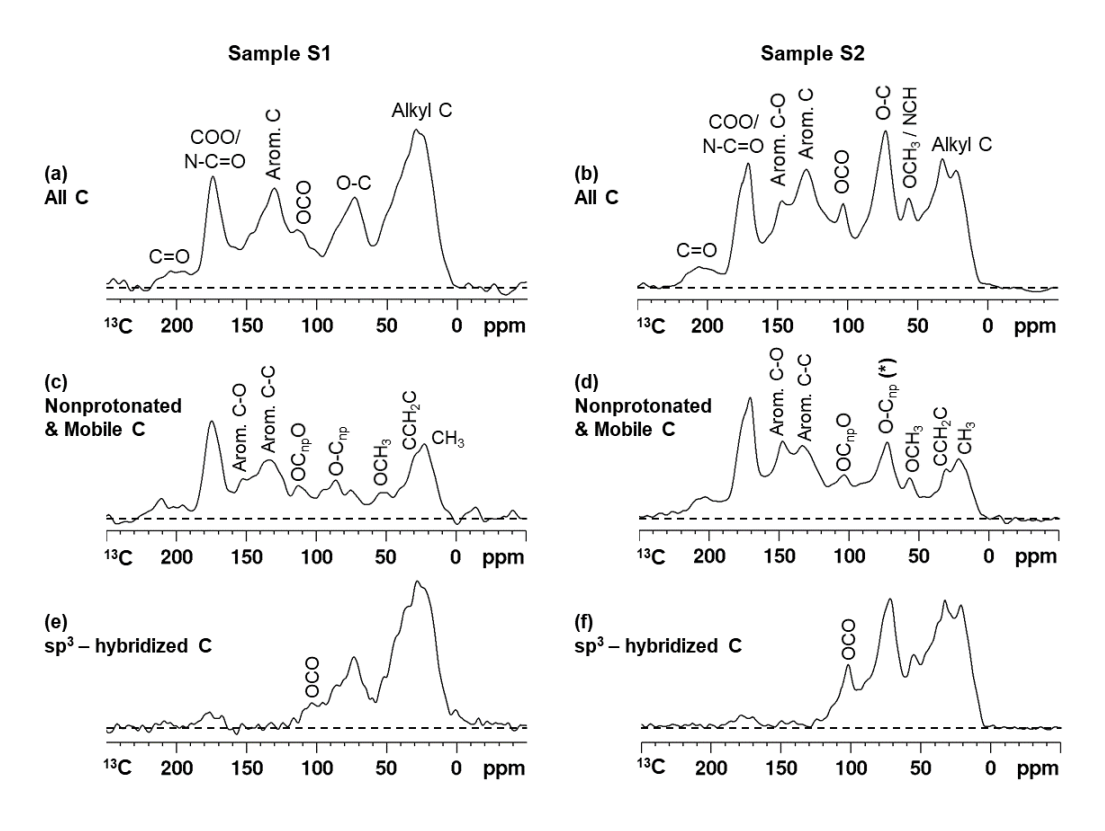


Figure 1. 13 C NMR with spectral editing of whole WSOM extracted from urban PM_{2.5} sample S1 [(a), (c), and (e)] and sample S2 [(b), (d), and (f)] collected in Aveiro. (a, b) Nearly quantitative multiCP/MAS 13 C NMR spectra (all carbon (C)), compared to the corresponding (c, d) dipolar-dephased 68- μ s multiCP/MAS 13 C NMR spectra of nonprotonated C (C_{np}) and highly mobile CH_n groups, and (e, f) selection of sp³-hybridized C signals by a 13 C CSA filter. The asterisk (*) in (d) denotes that the resonance at 62–94 ppm can have contributions of both O-C_{np} and highly mobile O-C(H,R')-C groups.

Table 2 lists the integrals of the NMR resonances of the specific functional groups identified in WSOM samples S1 and S2 by means of the multiCP and spectral-editing techniques as well as their ambient concentrations. The assignments are as follows: 0–49 ppm, alkyl carbon (C); 49–62 ppm, NCH and OCH₃; 62–94 ppm, O-alkyl C, including carbohydrate-like C; 94–110 ppm, O-C-O anomeric C; 110–141 ppm, aromatic C-C and C-H; 141–160 ppm, aromatic C-O; 160–188 ppm, COO and N-C=O;

and 188–230 ppm, ketone or aldehyde C. The spectra of multiCP/MAS ¹³C NMR combined with dipolar dephasing selected nonprotonated carbons and mobile functional groups, providing remarkable information on the type of potential functionalities within the two aerosol WSOM samples. The NMR data indicate that these samples hold similar carbon functional groups; however, they differ in terms of the relative carbon distribution.

Table 2. Integration results (percentage values) based on multiCP/MAS 13 C NMR and spectral editing techniques, and ambient concentrations (in μ g C m $^{-3}$) of each carbon functional group.

Sample ID	Chemical Shifts (ppm) and Assignments										
	230 188		160–141 Arom. C–O	141–110		110–94	94–62		62–49		49–0
	R(C=O)H R(C=O)R'			Arom. C-C	Arom. C-H	O-C(R,R')-O O-C(H,R')-O			OCH₃	NCH	CCH ₂ C CCH ₃
Percentage (%)											
S1	2.8	13.4	4.6	14.6	4.8	3.8	7.2	9.7	4.0	3.4	31.8
S2	3.6	12.4	8.4	15.4	2.9	6.9	10.5	9.5	3.8	2.3	24.3
Ambient	concentratio	n ^(a) (μg C r	n ⁻³)	<u> </u>				·	· 	·	<u> </u>
S1	0.09	0.44	0.15	0.48	0.16	0.13	0.24	0.32	0.13	0.11	1.06
S2	0.10	0.33	0.23	0.41	0.08	0.18	0.28	0.25	0.10	0.06	0.65

⁽a) Ambient concentration of each carbon functional group calculated based on the corresponding integration result (percentage value) and on the total amount of WSOC of the sample (shown in Table 1).

The spectrum of sample S1 is clearly dominated by the resonance assigned to alkyl C (31.8%), whereas the alkyl C (24.3%) and O-alkyl C (20.0%) resonances dominate the spectrum of sample S2 (Table 2). The NMR resonance assigned to carbohydrate-like moieties or other O-alkyls (62–94 ppm) is quite intense in both spectra (16.9 and 20.0%, respectively), particularly when compared to data obtained in previous conventional CP/MAS ¹³C NMR spectra of urban aerosol WSOM from cold seasons (10-12% of the total NMR peak area) (Duarte et al., 2015). The difference between these data and those previously published could be due to the different experimental procedures applied to WSOM processing (Duarte et al., 2015). Previously, the WSOM samples were isolated from the water-soluble inorganics using a solid-phase extraction (SPE) procedure (Duarte et al., 2015), whereas the present study focus on whole aerosol water-soluble extracts. It is suggested that the WSOM isolated using SPE is enriched in those organic species that are targeted by the low hydrophilic character of the SPE sorbent, which retains the highly conjugated and more hydrophobic compounds of the aerosol WSOM (Duarte et al.,

alkyl groups may contribute more than previously expected to the compositional features of whole aerosol WSOM in winter. The aromatic C structures (110-160 ppm), of which a substantial portion are nonprotonated aromatic C-C (14.6 and 15.4% in samples S1 and S2, respectively), also have an important contribution to the compositional features of both WSOM samples. However, a closer inspection of the multiCP/MAS ¹³C NMR data suggests that these aromatic C structures may have different origins in each sample. Note that the multiCP/MAS ¹³C spectra of both samples exhibit two distinctive NMR resonances at 56 ppm (OCH₃ and NCH) and 146 ppm (aromatic C-O; e.g., -OCH₃ or -OH substituents), whose presence are typically assigned to lignin breakdown products (e.g., methoxyphenols) emitted from wood combustion for home heating during cold temperatures (Duarte et al., 2017a, 2015; Matos et al., 2017). Nonetheless, the contribution of aromatic C-O groups to sample S2 is 1.8 times higher than for sample S1. Furthermore, the -OCH₃ and NCH groups contribute equally to the resonance at 56 ppm in sample S1, whereas a major fraction of this resonance is assigned to -OCH₃ groups in sample S2. Moreover, the content in anomeric C groups (94-110 ppm), whose presence is usually attributed to carbohydrate-like structures emitted during the pyrolysis of cellulose and hemi-cellulose (Duarte et al., 2019, 2008; Matos et al., 2017), is also higher in sample S2 than in sample S1. These spectral findings suggest that sample S1 is less wood smoke impacted than sample S2, although biomass burning still contributes to the composition of the former sample. The question is now which possible additional sources can explain the content of both aromatic C-C and C-H groups in sample S1. Motor-vehicle exhaust and secondary organic aerosol (SOA) formation have been mentioned as possible additional sources of aromatic C groups to urban aerosol WSOM (Chalbot et al., 2014; Sannigrahi et al., 2006). For example, aromatic acids, such as phthalic acid and its isomer, terephthalic acid, as well as nitrophenyl-derived compounds and cinnamic acid are water-soluble secondary products of oxidation of aromatic hydrocarbons from traffic emissions (Chalbot et al., 2016, 2014; Hallquist et al., 2009; Lee et al., 2014) and they have already been detected in aerosol WSOM samples in urban areas (Alier et al., 2013; Chalbot et al., 2016, 2014; Duarte et al., 2019, 2017a; Matos et al., 2017). Backward trajectories (Table S1) reveal that air masses transport from continental Europe was predominant during sample S1 collection, suggesting that the transport of polluted air masses from industrial and traffic-related urban sources (in addition to local sources) might contribute to the high aromatic C content of this WSOM sample. Fossil fuel

2015). The spectral features reported here further suggest that carbohydrate-like moieties or other O-

253

254

255

256

257

258

259

260

261

262

263

264

265

266

267

268

269

270

271

272

273

274

275

276

277

278

279

280

281

combustions are also major sources of aliphatic compounds in urban atmospheres (Willoughby et al., 2016; Wozniak et al., 2012). The presence of traffic and industrial activity in short- and long-range proximity of the sampling location suggests that fossil fuel combustion is also a strong candidate for explaining the high content of saturated aliphatic C groups (0-49 ppm) in sample S1 (Table 2). Approximately 17% (sample S1) to 20% (sample S2) of NMR signal intensity falls in the O-alkyl C region (62-94 ppm). Nevertheless, the estimates of protonated and nonprotonated O-alkyl C structures (Table 2) resonating within this region should be viewed with caution, as an uncounted fraction of O-C(H,R')-C resonating at ~73 ppm is highly mobile due to sample hygroscopicity. The O-alkyl C region is typically assigned to carbohydrate-like moieties, although other alcohols (polyols) can resonate within this region as well. Polyols have already been detected in urban aerosol WSOM (Fu et al., 2010; Minguillón et al., 2016; Suzuki et al., 2001; Wang and Kawamura, 2005) and are thought to be produced via photooxidation of isoprene in aerosols (e.g., 2-methyltetrols) (Fu et al., 2010; Minguillón et al., 2016). Carbohydrate-like moieties, on the other hand, are important components of aerosol WSOM and may include mono- and disaccharides (such as glucose, trehalose, maltose, fructose, and sucrose) and anhydrosugars (such as levoglucosan and mannosan) (Matos et al., 2017; Yttri et al., 2007). Glucose, fructose, maltose, and sucrose can be emitted from the combustion of cellulose and hemi-cellulose, whereas anhydrosugars are molecular markers of biomass burning emissions (Chalbot et al., 2013; Duarte et al., 2019, 2008; Matos et al., 2017). Primary saccharides, such as glucose and trehalose, may also reflect the contribution of biogenic sources (e.g., products of fungal metabolism) (Côté et al., 2008). Trehalose is considered a useful tracer of soil materials and associated microbiota (Simoneit et al., 2004) and, therefore, resuspension of soil from agricultural activities in areas near the sampling area could be a plausible source as well. Interestingly, the content in NCH groups, which overlap with those of -OCH3 groups in the multiCP ¹³C NMR spectra and are removed by dipolar dephasing (Mao et al., 2012), is somewhat higher in sample S1 than in sample S2 (Table 2). The presence of N-alkyl structures has already been identified in aerosol WSOM samples (Matos et al., 2017), but their quantification in organic aerosols is rather difficult. These N-containing organic structures could be associated with SOA formation, resulting from photochemical oxidation of different anthropogenic and natural gas-phase precursors (e.g., alkanes, carbonyl, aliphatic amines, epoxides, and anhydrides) (Duarte et al., 2019; Matos et al., 2017). The long-range transport

283

284

285

286

287

288

289

290

291

292

293

294

295

296

297

298

299

300

301

302

303

304

305

306

307

308

309

310

of polluted air masses from inland urban and industrial sources (Table S1) can contribute to the higher content of these N-containing structures in sample S1 as compared to sample S2.

In both samples, the dipolar-dephased spectra also exhibit signals from -COO and N-C=O between 160-188 ppm, and ketones between 188-230 ppm. Apparently, the presence of aldehydes C groups (188-230 ppm) is not significant for both WSOM samples, since the corresponding dipolar-dephased spectra do not show a considerable signal decrease within this spectral region.

318

319

320

321

322

323

324

325

326

327

328

329

330

331

332

333

334

335

336

337

338

339

340

312

313

314

315

316

317

3.3. Structural information on aerosol WSOM from 2D HETCOR NMR

To further assess the connectivities (or proximities) of the different C functional groups, the 2D HETCOR spectrum of sample S2 was also acquired [Figure 2(a)]. The ¹H cross sections at specific ¹³C chemical shifts were extracted to facilitate the identification of connectivities and/or proximities of different functional groups [Figure 2(b)]. The ¹H cross sections extracted at the alkyl ¹³C chemical shifts of 21 and 33 ppm, attributable to mobile -CH₃ and CCH₂C groups, respectively, show that the dominant contributions are from alkyl ¹H at 1.2 ppm, although proximity to aromatic ¹H at 7.1 ppm is also observed, particularly for alkyl ¹³C at 21 ppm. While the former feature indicates that polymethylene structures and terminal CH₃ are important contributors to WSOM, the latter indicates that neutral alkyl C groups (namely CH₃) might be also substituents in aromatic rings. The ¹H slice extracted at 42 ppm, likely from -CCHC and/or quaternary C groups, mainly show correlation with alkyl ¹H at 1.9 ppm, indicating that aliphatic structures in the WSOM sample may also include branched carbon chains. The ¹H spectrum associated with OCH₃/NCH groups at 55 ppm indicates that these carbons are mainly associated with their directly bonded ¹H at 3.25 ppm, although their proximity with aromatic ¹H resonating at ≈8.0 ppm is also observed. Considering that -OCH₃ groups account for most of the resonance within the 49-62 ppm region (Table 2), these spectral features are consistent with the presence of lignin-derived structures, which are a defining feature of biomass burning emissions and of importance in the composition of sample S2. The ¹H slice at the ¹³C chemical shift of 71 ppm, assigned to -OCH groups, show mainly an O-alkyl ¹H band at 3.9 ppm, suggesting that these carbon sites primarily correlate with their directly bonded O-alkyl ¹H. Furthermore, the ¹H slice extracted at 102 ppm also indicates that the protonated anomeric C (O-C-O) shows correlations predominantly with anomeric ¹H resonating at 4.7 ppm. These findings confirm that both -OCH and O-C-O are primarily associated with

carbohydrate-like moieties, whose presence in this sample may result from cellulose and hemicellulose combustion.

341

342

343

344345

346

347

348

349

350

351

352

353

354

355

356

357

358

359

360

361

362

363

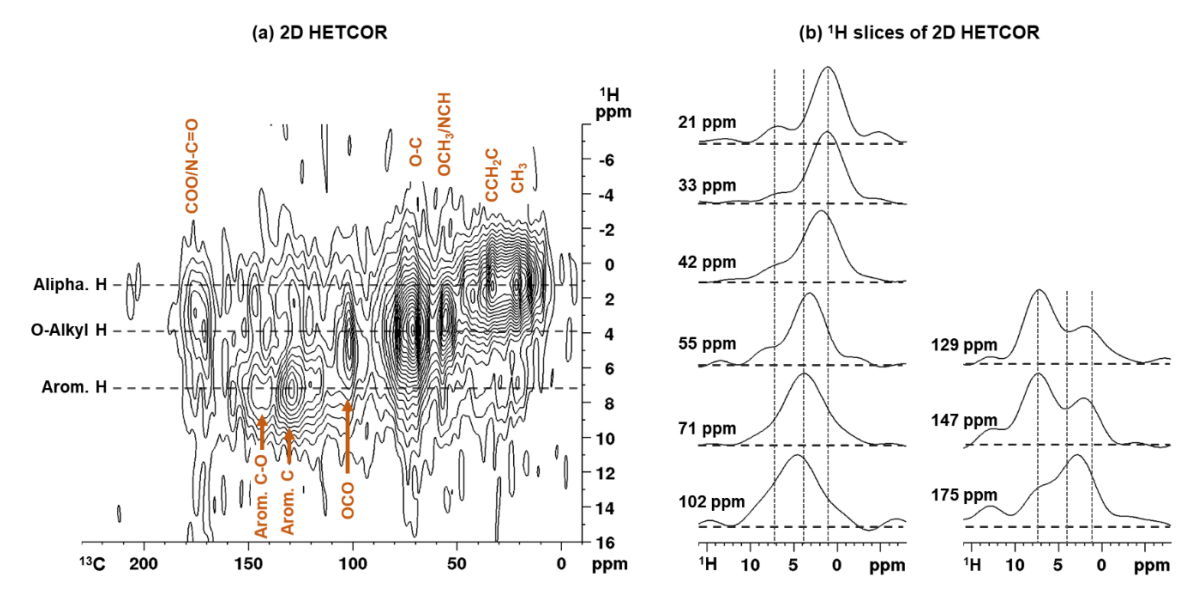


Figure 2. 2D $^{1}H-^{13}C$ HETCOR NMR spectrum (a) and associated ^{1}H slices (b) of whole WSOM extracted from PM_{2.5} sample S2.

Within the aromatic NMR region, the ¹H slices extracted at the chemical shifts of aromatic C (129 ppm) and aromatic C-O (147 ppm) show major contributions from aromatic ¹H (at ≈7.3 ppm) as well as signals of alkyl ¹H (at ≈2.0 ppm). Aromatic C-O is also correlated with carboxylic acid ¹H at 12 ppm. These NMR fingerprints suggest the presence of highly substituted aromatic rings, bearing neutral (alkyl C) and/or O-containing (namely, OCH₃, OH, and/or COOR, where R=H or alkyl group) substituents. Such aromatic structural signatures are consistent with those observed for molecular markers of primary organic aerosols that are directly emitted from biomass burning (Duarte et al., 2019, 2008; Matos et al., 2017). Their presence in sample S2 confirm the importance of this emission source in the chemical composition of this aerosol WSOM sample during winter. Additional sources contributing to the aromatic structural signatures of sample S2 can also include in-situ secondary formation, as the presence of COO-bonded aromatics has been associated to terephthalic acid and cinnamic acid, possibly formed during the oxidation of aromatic hydrocarbons from urban traffic emissions (Duarte et al., 2019; Matos et al., 2017). The 2D HETCOR spectrum also shows that COO/N-C=O groups (175 ppm), which account to 12% of the NMR signal (Table 2), are primarily correlated with alkyl ¹H at 2.8 ppm, with additional contributions from O-alkyl, aromatic and carboxylic acid ¹H. The presence of COO groups bonded to alkyls, O-alkyls, and aromatic structures in urban aerosol WSOM can be attributed to SOA that form via oxidation reactions involving naturally (e.g., sea-to-air emission of marine organics, and terrestrial vegetation (Liu et al., 2011; Russell et al., 2011; Schmitt-Kopplin et al., 2012)) and anthropogenically (e.g., biomass burning and fossil fuel combustion (Kundu et al., 2010; Liu et al., 2011)) gas-phase precursors. In the context of the studied urban area, the contribution of fossil fuel SOA to total organic aerosol load has a noteworthy importance in winter (up to 20% of the total aerosol carbon (Gelencsér et al., 2007)), thus making atmospheric aging of anthropogenic volatile and semi-volatile organic compounds a key process in defining the molecular features of urban organic aerosols.

A structural model of aerosol WSOM can be further deduced based on the data from multiCP/MAS ¹³C NMR with spectral editing techniques (Table 2) and 2D HETCOR. Figure 3 integrates all the structural information on the complex molecular WSOM assemblies, with the addition of the chemical data from 2D solution-state NMR of urban organic aerosols (Duarte et al., 2019, 2017a; Matos et al., 2017). The model shows that urban particulate WSOM contain at least three classes of compounds which are not associated with each other in the same structure, and that vary both in concentration and molecular diversity within short periods of time: (1) a core of heteroatom-rich aliphatics (either chain or branched, mostly with -CH₃ and/or -COO terminal units), reflecting the large contribution of these structures as deduced from the quantitative NMR data in Table 2; (2) carbohydrate-like moieties; and (3) highly substituted aromatic units.



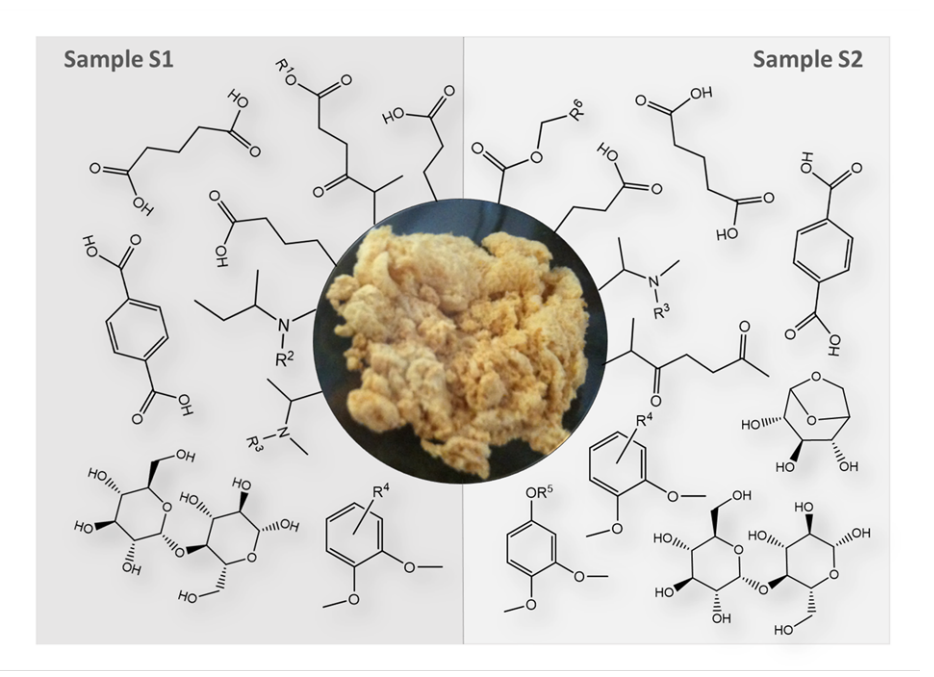


Figure 3. Structural model of aerosol WSOM in samples S1 and S2, with a ratio of aliphatic -CH₃, C-CH₂-C, -COO, aromatic C-O, and anomeric O-C-O of 5:11:7:2:2 and 4:8:6:4:3, respectively, as deduced from the combination of multiCP/MAS 13 C NMR with spectral editing techniques and 2D HETCOR (R¹ to R⁶ = H or alkyl group; photo: aerosol WSOM, after freeze-drying).

386

387

388

389

390

391

392

393

394

395

396

397

398

399

400

401

402

403

404

405

406

407

408

409

410

411

412

413

414

415

4. Conclusions

The combination of multiCP/MAS ¹³C NMR with spectral editing techniques has been critical in providing, for the first time, key information on the major and specific structural components of whole WSOM present in urban PM_{2.5} collected in two short periods of time. The weekly-resolved structural data show quantifiable changes in whole aerosol WSOM composition not observable until now in NMR datasets provided in the literature. The O- and N-containing aliphatic features of sample S1 may reflect the effect of long-range-transported anthropogenic emissions (namely, from fossil-fuel combustion sources) that underwent chemical aging along the transport. These aged anthropogenic emissions might also contribute to the aromatic C features of sample S1. However, local residential wood burning also contributes to the WSOM composition to a minor extent. On the other hand, the structural characteristics of sample S2, particularly the carbohydrate-like and the highly substituted aromatic moieties, are mainly apportioned to local biomass burning emissions. SOA formation from anthropogenic precursors emitted from local traffic sources can also contribute to whole aerosol WSOM during the second week. The knowledge on the whole aerosol WSOM functional-group composition should also be helpful for predicting the role of this fraction in diverse atmospheric processes. Rather than using surrogate organic compounds to represent aerosol WSOM, improved reproductions of how WSOM affect aerosol hygroscopic growth and activation should be obtained if accurate ambient concentrations of each carbon functional group (Table 2) are appropriately taken into account in such modelling studies (McNeill, 2015; Mircea et al., 2005). Our structural findings further highlight a dynamic picture of aerosol WSOM composition that should be integrated in climate models. For example, Martin and co-workers reported that it is not possible to use the same value of hygroscopicity for freshly emitted and aged soot particles in climate models due to their different chemical composition (Martin et al., 2013). Therefore, it is worth investigating how the hygroscopic properties change relative to the different composition of locally emitted primary organic aerosols and chemically processed organic particles, as this would make the inferred values in climate models more representative. Future research should refine both the composition and structures of whole aerosol WSOM by addressing additional sample sets from other locations across different time scales, which should enable a more definite quantification and better constrained structural models of this organic aerosol fraction.

The application of advanced solid-state ¹³C NMR methods will lay the groundwork for such structure—

function investigations, thus enabling exploration of role of WSOM in different atmospheric processes.

419

420

416

417

418

Acknowledgments

- Thanks are due to FCT/MCTES for the financial support to CESAM (UID/AMB/50017/2019) and project
 AMBIEnCE (PTDC/CTA-AMB/28582/2017), through national funds. Regina Duarte also acknowledges
 financial support from FCT/MCTES (Investigator FCT Contract IF/00798/2015) and from the Fulbright
 Scholar Program (sponsored by the U.S. Department of State), as well as the Surface Ocean-Lower
 Atmosphere Study (SOLAS) for endorsing the AMBIEnCE project. The solid-state NMR spectrometer
 used in this work was funded by the NSF (Award No. 1726346). The authors also gratefully acknowledge
- 427 the NOAA Air Resources Laboratory (ARL) for the provision of the HYSPLIT transport and dispersion
- 428 model and/or READY website (http://www.ready.noaa.gov) used in this publication.

429

430

References

- 431 Alier, M., Van Drooge, B.L., Dall'Osto, M., Querol, X., Grimalt, J.O., Tauler, R., 2013. Source
- apportionment of submicron organic aerosol at an urban background and a road site in Barcelona
- 433 (Spain) during SAPUSS. Atmospheric Chemistry and Physics 13, 10353–10371.
- 434 https://doi.org/10.5194/acp-13-10353-2013
- Chalbot, M.-C., Nikolich, G., Etyemezian, V., Dubois, D.W., King, J., Shafer, D., Gamboa da Costa, G.,
- Hinton, J.F., Kavouras, I.G., 2013. Soil humic-like organic compounds in prescribed fire emissions
- using nuclear magnetic resonance spectroscopy. Environmental Pollution 181, 167–171.
- 438 https://doi.org/10.1016/j.envpol.2013.06.008
- Chalbot, M.-C.G., Brown, J., Chitranshi, P., Gamboa da Costa, G., Pollock, E.D., Kavouras, I.G., 2014.
- 440 Functional characterization of the water-soluble organic carbon of size-fractionated aerosol in the
- southern Mississippi Valley. Atmospheric Chemistry and Physics 14, 6075–6088.
- 442 https://doi.org/10.5194/acp-14-6075-2014
- Chalbot, M.-C.G., Chitranshi, P., Gamboa da Costa, G., Pollock, E., Kavouras, I.G., 2016.
- Characterization of water-soluble organic matter in urban aerosol by 1H-NMR spectroscopy.
- 445 Atmospheric Environment 128, 235–245. https://doi.org/10.1016/j.atmosenv.2015.12.067

- Côté, V., Kos, G., Mortazavi, R., Ariya, P.A., 2008. Microbial and "de novo" transformation of dicarboxylic
- acids by three airborne fungi. Science of the Total Environment 390, 530-537.
- 448 https://doi.org/10.1016/j.scitotenv.2007.10.035
- Duarte, R.M.B.O., Duarte, A.C., 2017. NMR Studies of Organic Aerosols, in: Webb, G.A. (Ed.), Annual
- 450 Reports on NMR Spectroscopy. Academic Press, Oxford, pp. 83-135.
- 451 https://doi.org/10.1016/bs.arnmr.2017.04.003
- Duarte, R.M.B.O., Duarte, A.C., 2015. Unraveling the structural features of organic aerosols by NMR
- 453 spectroscopy: a review. Magnetic Resonance in Chemistry 53, 658–666.
- 454 https://doi.org/10.1002/mrc.4227
- Duarte, R.M.B.O., Duarte, A.C., 2011. A critical review of advanced analytical techniques for water-
- 456 soluble organic matter from atmospheric aerosols. TrAC Trends in Analytical Chemistry 30, 1659–
- 457 1671. https://doi.org/10.1016/j.trac.2011.04.020
- Duarte, R.M.B.O., Freire, S.M.S.C., Duarte, A.C., 2015. Investigating the water-soluble organic
- functionality of urban aerosols using two-dimensional correlation of solid-state 13C NMR and FTIR
- 460 spectral data. Atmospheric Environment 116, 245–252.
- 461 https://doi.org/10.1016/j.atmosenv.2015.06.043
- 462 Duarte, R.M.B.O., Matos, J.T.V., Paula, A.S., Lopes, S.P., Pereira, G., Vasconcellos, P., Gioda, A.,
- 463 Carreira, R., Silva, A.M.S., Duarte, A.C., Smichowski, P., Rojas, N., Sanchez-Ccoyllo, O., 2017a.
- 464 Structural signatures of water-soluble organic aerosols in contrasting environments in South
- 465 America and Western Europe. Environmental Pollution 227, 513–525.
- 466 https://doi.org/10.1016/j.envpol.2017.05.011
- Duarte, R.M.B.O., Matos, J.T.V., Paula, A.S., Lopes, S.P., Ribeiro, S., Santos, J.F., Patinha, C., da
- Silva, E.F., Soares, R., Duarte, A.C., 2017b. Tracing of aerosol sources in an urban environment
- 469 using chemical, Sr isotope, and mineralogical characterization. Environmental Science and
- 470 Pollution Research 24, 11006–11016. https://doi.org/10.1007/s11356-016-7793-8
- Duarte, R.M.B.O., Piñeiro-Iglesias, M., López-Mahía, P., Muniategui-Lorenzo, S., Moreda-Piñeiro, J.,
- Silva, A.M.S., Duarte, A.C., 2019. Comparative study of atmospheric water-soluble organic
- 473 aerosols composition in contrasting suburban environments in the Iberian Peninsula Coast.
- 474 Science of the Total Environment 648, 430–441. https://doi.org/10.1016/j.scitotenv.2018.08.171
- 475 Duarte, R.M.B.O., Pio, C.A., Duarte, A.C., 2005. Spectroscopic study of the water-soluble organic matter

- 476 isolated from atmospheric aerosols collected under different atmospheric conditions. Analytica
- 477 Chimica Acta 530, 7–14. https://doi.org/10.1016/j.aca.2004.08.049
- Duarte, R.M.B.O., Santos, E.B.H., Pio, C.A., Duarte, A.C., 2007. Comparison of structural features of
- water-soluble organic matter from atmospheric aerosols with those of aquatic humic substances.
- 480 Atmospheric Environment 41, 8100–8113. https://doi.org/10.1016/j.atmosenv.2007.06.034
- Duarte, R.M.B.O., Silva, A.M.S., Duarte, A.C., 2008. Two-Dimensional NMR Studies of Water-Soluble
- Organic Matter in Atmospheric Aerosols. Environmental Science & Technology 42, 8224–8230.
- 483 https://doi.org/Doi 10.1021/Es801298s
- 484 Fu, P.Q., Kawamura, K., Pavuluri, C.M., Swaminathan, T., Chen, J., 2010. Molecular characterization
- of urban organic aerosol in tropical India: Contributions of primary emissions and secondary
- photooxidation. Atmospheric Chemistry and Physics 10, 2663–2689. https://doi.org/10.5194/acp-
- 487 10-2663-2010
- 488 Gelencsér, A., May, B., Simpson, D., Sánchez-Ochoa, A., Kasper-Giebl, A., Puxbaum, H., Caseiro, A.,
- 489 Pio, C.A., Legrand, M., 2007. Source apportionment of PM2.5 organic aerosol over Europe:
- 490 Primary/secondary, natural/anthropogenic, and fossil/biogenic origin. Journal of Geophysical
- 491 Research Atmospheres 112, 1–12. https://doi.org/10.1029/2006JD008094
- 492 George, C., Ammann, M., D'Anna, B., Donaldson, D.J., Nizkorodov, S.A., 2015. Heterogeneous
- 493 photochemistry in the atmosphere. Chemical Reviews 115, 4218–4258.
- 494 https://doi.org/10.1021/cr500648z
- 495 Hallquist, M., Wenger, J.C., Baltensperger, U., Rudich, Y., Simpson, D., Claeys, M., Dommen, J.,
- Donahue, N.M., George, C., Goldstein, A.H., Hamilton, J.F., Herrmann, H., Hoffmann, T., Iinuma,
- 497 Y., Jang, M., Jenkin, M.E., Jimenez, J.L., Kiendler-Scharr, A., Maenhaut, W., McFiggans, G.,
- 498 Mentel, T.F., Monod, A., Prévôt, A.S.H., Seinfeld, J.H., Surratt, J.D., Szmigielski, R., Wildt, J.,
- 499 2009. The formation, properties and impact of secondary organic aerosol: current and emerging
- issues. Atmospheric Chemistry and Physics 9, 5155-5236. https://doi.org/10.5194/acp-9-5155-
- 501 2009
- 502 lavorivska, L., Boyer, E.W., DeWalle, D.R., 2016. Atmospheric deposition of organic carbon via
- 503 precipitation. Atmospheric Environment 146, 153–163.
- 504 https://doi.org/10.1016/j.atmosenv.2016.06.006
- Johnson, R.L., Schmidt-Rohr, K., 2014. Quantitative solid-state13C NMR with signal enhancement by

- 506 multiple cross polarization. Journal of Magnetic Resonance 239, 44-49.
- 507 https://doi.org/10.1016/j.jmr.2013.11.009
- Kundu, S., Kawamura, K., Andreae, T.W., Hoffer, A., Andreae, M.O., 2010. Molecular distributions of
- 509 dicarboxylic acids, ketocarboxylic acids and α-dicarbonyls in biomass burning aerosols:
- 510 implications for photochemical production and degradation in smoke layers. Atmospheric
- 511 Chemistry and Physics 10, 2209–2225. https://doi.org/10.5194/acp-10-2209-2010
- Laskin, A., Laskin, J., Nizkorodov, S.A., 2015. Chemistry of Atmospheric Brown Carbon. Chemical
- 513 Reviews 115, 4335–4382. https://doi.org/10.1021/cr5006167
- Lee, H.J. (Julie), Aiona, P.K., Laskin, A., Laskin, J., Nizkorodov, S.A., 2014. Effect of Solar Radiation on
- 515 the Optical Properties and Molecular Composition of Laboratory Proxies of Atmospheric Brown
- 516 Carbon. Environmental Science & Technology 48, 10217–10226.
- 517 https://doi.org/10.1021/es502515r
- Liu, S., Day, D.A., Shields, J.E., Russell, L.M., 2011. Ozone-driven daytime formation of secondary
- organic aerosol containing carboxylic acid groups and alkane groups. Atmospheric Chemistry and
- 520 Physics 11, 8321–8341. https://doi.org/10.5194/acp-11-8321-2011
- Mao, J., Cao, X., Olk, D.C., Chu, W., Schmidt-Rohr, K., 2017. Advanced solid-state NMR spectroscopy
- of natural organic matter. Progress in Nuclear Magnetic Resonance Spectroscopy 100, 17–51.
- 523 https://doi.org/10.1016/j.pnmrs.2016.11.003
- 524 Mao, J., Chen, N., Cao, X., 2011. Characterization of humic substances by advanced solid state NMR
- 525 spectroscopy: Demonstration of a systematic approach. Organic Geochemistry 42, 891–902.
- 526 https://doi.org/10.1016/j.orggeochem.2011.03.023
- Mao, J., Kong, X., Schmidt-Rohr, K., Pignatello, J.J., Perdue, E.M., 2012. Advanced solid-state NMR
- 528 characterization of marine dissolved organic matter isolated using the coupled reverse
- 529 osmosis/electrodialysis method. Environmental Science and Technology 46, 5806–5814.
- 530 https://doi.org/10.1021/es300521e
- Mao, J.D., Schmidt-Rohr, K., 2004a. Accurate Quantification of Aromaticity and Nonprotonated Aromatic
- 532 Carbon Fraction in Natural Organic Matter by 13C Solid-State Nuclear Magnetic Resonance.
- 533 Environmental Science and Technology 38, 2680–2684. https://doi.org/10.1021/es034770x
- 534 Mao, J.D., Schmidt-Rohr, K., 2004b. Separation of aromatic-carbon13C NMR signals from di-
- oxygenated alkyl bands by a chemical-shift-anisotropy filter. Solid State Nuclear Magnetic

- 536 Resonance 26, 36–45. https://doi.org/10.1016/j.ssnmr.2003.09.003
- 537 Mao, J.D., Xing, B., Schmidt-Rohr, K., 2001. New Structural Information on a Humic Acid from Two-
- 538 Dimensional 1 H- 13 C Correlation Solid-State Nuclear Magnetic Resonance. Environmental
- 539 Science & Technology 35, 1928–1934. https://doi.org/10.1021/es0014988
- Martin, M., Tritscher, T., Jurányi, Z., Heringa, M.F., Sierau, B., Weingartner, E., Chirico, R., Gysel, M.,
- Prévôt, A.S.H., Baltensperger, U., Lohmann, U., 2013. Hygroscopic properties of fresh and aged
- 542 wood burning particles. Journal of Aerosol Science 56, 15–29.
- 543 https://doi.org/10.1016/j.jaerosci.2012.08.006
- Matos, J.T.V., Duarte, R.M.B.O., Lopes, S.P., Silva, A.M.S., Duarte, A.C., 2017. Persistence of urban
- organic aerosols composition: Decoding their structural complexity and seasonal variability.
- 546 Environmental Pollution 231, 281–290. https://doi.org/10.1016/j.envpol.2017.08.022
- McNeill, V.F., 2015. Aqueous organic chemistry in the atmosphere: Sources and chemical processing
- of organic aerosols. Environmental Science and Technology 49, 1237–1244.
- 549 https://doi.org/10.1021/es5043707
- Minguillón, M.C., Pérez, N., Marchand, N., Bertrand, A., Temime-Roussel, B., Agrios, K., Szidat, S., van
- Drooge, B., Sylvestre, A., Alastuey, A., Reche, C., Ripoll, A., Marco, E., Grimalt, J.O., Querol, X.,
- 552 2016. Secondary organic aerosol origin in an urban environment: influence of biogenic and fuel
- combustion precursors. Faraday Discuss. 189, 337–359. https://doi.org/10.1039/C5FD00182J
- 554 Mircea, M., Facchini, M.C., Decesari, S., Cavalli, F., Emblico, L., Fuzzi, S., Vestin, A., Rissler, J.,
- Swietlicki, E., Frank, G., Andreae, M.O., Maenhaut, W., Rudich, Y., Artaxo, P., 2005. Importance
- of the organic aerosol fraction for modeling aerosol hygroscopic growth and activation: A case
- 557 study in the Amazon Basin. Atmospheric Chemistry and Physics 5, 3111–3126.
- 558 https://doi.org/10.5194/acp-5-3111-2005
- Moise, T., Flores, J.M., Rudich, Y., 2015. Optical properties of secondary organic aerosols and their
- 560 changes by chemical processes. Chemical Reviews 115, 4400–4439.
- 561 https://doi.org/10.1021/cr5005259
- Müller, A., Miyazaki, Y., Tachibana, E., Kawamura, K., Hiura, T., 2017. Evidence of a reduction in cloud
- 563 condensation nuclei activity of water-soluble aerosols caused by biogenic emissions in a coolerate
- 564 forest. Scientific Reports 7, 1–9. https://doi.org/10.1038/s41598-017-08112-9
- Nozière, B., Kalberer, M., Claeys, M., Allan, J., D'Anna, B., Decesari, S., Finessi, E., Glasius, M., Grgić,

- I., Hamilton, J.F., Hoffmann, T., Iinuma, Y., Jaoui, M., Kahnt, A., Kampf, C.J., Kourtchev, I.,
- Maenhaut, W., Marsden, N., Saarikoski, S., Schnelle-Kreis, J., Surratt, J.D., Szidat, S.,
- Szmigielski, R., Wisthaler, A., 2015. The molecular identification of organic compounds in the
- atmosphere: State of the art and challenges. Chemical Reviews 115, 3919–3983.
- 570 https://doi.org/10.1021/cr5003485
- Padró, L.T., Tkacik, D., Lathem, T., Hennigan, C.J., Sullivan, A.P., Weber, R.J., Huey, L.G., Nenes, A.,
- 572 2010. Investigation of cloud condensation nuclei properties and droplet growth kinetics of the
- 573 water-soluble aerosol fraction in Mexico City. Journal of Geophysical Research 115, D09204.
- 574 https://doi.org/10.1029/2009JD013195
- Russell, L.M., Bahadur, R., Ziemann, P.J., 2011. Identifying organic aerosol sources by comparing
- functional group composition in chamber and atmospheric particles. Proceedings of the National
- 577 Academy of Sciences 108, 3516–3521. https://doi.org/10.1073/pnas.1006461108
- 578 Sannigrahi, P., Sullivan, A.P., Weber, R.J., Ingall, E.D., 2006. Characterization of water-soluble organic
- 579 carbon in urban atmospheric aerosols using solid-state C-13 NMR spectroscopy. Environmental
- Science & Technology 40, 666–672. https://doi.org/Doi 10.1021/Es051150i
- 581 Schmitt-Kopplin, P., Gelencsér, A., Dabek-Zlotorzynska, E., Kiss, G., Hertkorn, N., Harir, M., Hong, Y.,
- 582 Gebefügi, I., 2010. Analysis of the Unresolved Organic Fraction in Atmospheric Aerosols with
- 583 Ultrahigh-Resolution Mass Spectrometry and Nuclear Magnetic Resonance Spectroscopy:
- 584 Organosulfates As Photochemical Smog Constituents. Analytical Chemistry 82, 8017–8026.
- 585 https://doi.org/10.1021/ac101444r
- 586 Schmitt-Kopplin, P., Liger-Belair, G., Koch, B.P., Flerus, R., Kattner, G., Harir, M., Kanawati, B., Lucio,
- 587 M., Tziotis, D., Hertkorn, N., Gebefügi, I., 2012. Dissolved organic matter in sea spray: a transfer
- 588 study from marine surface water to aerosols. Biogeosciences 9, 1571–1582.
- 589 https://doi.org/10.5194/bg-9-1571-2012
- 590 Simoneit, B.R.T., Elias, V.O., Kobayashi, M., Kawamura, K., Rushdi, A.I., Medeiros, P.M., Rogge, W.F.,
- 591 Didyk, B.M., 2004. Sugars Dominant water-soluble organic compounds in soils and
- 592 characterization as tracers in atmospheric participate matter. Environmental Science and
- 593 Technology 38, 5939–5949. https://doi.org/10.1021/es0403099
- 594 Simpson, A.J., McNally, D.J., Simpson, M.J., 2011. NMR spectroscopy in environmental research: From
- 595 molecular interactions to global processes. Progress in Nuclear Magnetic Resonance

596	Spectroscopy 58, 97–175. https://doi.org/10.1016/j.pnmrs.2010.09.001
597	Suzuki, Y., Kawakami, M., Akasaka, K., 2001. 1H NMR application for characterizing water-soluble
598	organic compounds in urban atmospheric particles. Environmental Science and Technology 35,
599	2656–2664. https://doi.org/10.1021/es001861a
600	Tuet, W.Y., Fok, S., Verma, V., Tagle Rodriguez, M.S., Grosberg, A., Champion, J.A., Ng, N.L., 2016.
601	Dose-dependent intracellular reactive oxygen and nitrogen species (ROS/RNS) production from
602	particulate matter exposure: comparison to oxidative potential and chemical composition.
603	Atmospheric Environment 144, 335–344. https://doi.org/10.1016/j.atmosenv.2016.09.005
604	Verma, V., Fang, T., Guo, H., King, L., Bates, J.T., Peltier, R.E., Edgerton, E., Russell, A.G., Weber,
605	R.J., 2014. Reactive oxygen species associated with water-soluble PM2.5 in the southeastern
606	United States: spatiotemporal trends and source apportionment. Atmospheric Chemistry and
607	Physics 14, 12915–12930. https://doi.org/10.5194/acp-14-12915-2014
608	Wang, G., Kawamura, K., 2005. Molecular Characteristics of Urban Organic Aerosols from Nanjing A
609	Case Study of A Mega-City in China. Environmental Science & Technology 39, 7430-7438.
610	https://doi.org/10.1021/es051055
611	Willoughby, A.S., Wozniak, A.S., Hatcher, P.G., 2016. Detailed source-specific molecular composition
612	of ambient aerosol organic matter using ultrahigh resolution mass spectrometry and 1H NMR.
613	Atmosphere 7. https://doi.org/10.3390/atmos7060079
614	Witkowska, A., Lewandowska, A., Falkowska, L.M., 2016. Parallel measurements of organic and
615	elemental carbon dry (PM1, PM2.5) and wet (rain, snow, mixed) deposition into the Baltic Sea.
616	Marine Pollution Bulletin 104, 303–312. https://doi.org/10.1016/j.marpolbul.2016.01.003
617	Wozniak, A.S., Bauer, J.E., Dickhut, R.M., 2012. Characteristics of water-soluble organic carbon
618	associated with aerosol particles in the eastern United States. Atmospheric Environment 46, 181-
619	188. https://doi.org/10.1016/j.atmosenv.2011.10.001
620	Yttri, K.E., Dye, C., Kiss, G., 2007. Ambient aerosol concentrations of sugars and sugar-alcohols at four
621	different sites in Norway. Atmospheric Chemistry and Physics 7, 4267–4279.
622	https://doi.org/10.5194/acp-7-4267-2007
623	

FIGURES CAPTIONS

- Figure 1. ¹³C NMR with spectral editing of whole WSOM extracted from urban PM_{2.5} sample S1 [(a), (c), and (e)] and sample S2 [(b), (d), and (f)] collected in Aveiro. (a, b) Nearly quantitative multiCP/MAS ¹³C NMR spectra (all carbon (C)), compared to the corresponding (c, d) dipolar-dephased 68-μs multiCP/MAS ¹³C NMR spectra of nonprotonated C (C_{np}) and highly mobile CH_n groups, and (e, f) selection of sp³-hybridized C signals by a ¹³C CSA filter. The asterisk (*) in (d) denotes that the resonance at 62–94 ppm can have contributions of both O-C_{np} and highly mobile O–C(H,R')–C groups.
 - **Figure 2.** 2D ¹H-¹³C HETCOR NMR spectrum (a) and associated ¹H slices (b) of whole WSOM extracted from PM_{2.5} sample S2.
- **Figure 3.** Structural model of aerosol WSOM in samples S1 and S2, with a ratio of aliphatic -CH₃, C-CH₂-C, -COO, aromatic C-O, and anomeric O-C-O of 5:11:7:2:2 and 4:8:6:4:3, respectively, as deduced from the combination of multiCP/MAS ¹³C NMR with spectral editing techniques and 2D HETCOR (R¹ to R⁶ = H or alkyl group; photo: aerosol WSOM, after freeze-drying).